

Article

Feasibility of Behind-the-Meter Battery Storage in Wind Farms Operating on Small Islands

Pantelis A. Dratsas ^{*}, Georgios N. Psarros  and Stavros A. Papathanassiou ^{*}

School of Electrical and Computer Engineering, National Technical University of Athens (NTUA), Zografou Campus, 9, Iroon Polytechniou Str., 15780 Athens, Greece

^{*} Correspondence: pantelisdatsas@mail.ntua.gr (P.A.D.); st@power.ece.ntua.gr (S.A.P.)

Abstract: This paper investigates the anticipated benefits from the introduction of a battery energy storage system (BESS) behind-the-meter (BtM) of a wind farm (WF) located in a small non-interconnected island (NII) system. Contrary to the standard storage deployment applications for NII, where storage is either installed in front of the meter as a system asset or integrated into a virtual power plant with renewable energy sources, the BESS of this paper is utilized to manage the power injection constraints imposed on the WF, aiming to minimize wind energy curtailments and improve WF's yield. A mixed integer linear programming generation scheduling model is used to simulate the operation of the system and determine the permissible wind energy absorption margin. Then, a self-dispatch algorithm is employed for the operation of the WF-BESS facility, using the BESS to manage excess wind generation that cannot be directly delivered to the grid. Additionally, the contribution of BESS to the capacity adequacy of the NII system is investigated using a Monte Carlo-based probabilistic model, amended appropriately to incorporate storage. Finally, an economic feasibility analysis is carried out, considering the possible revenue streams. By examining several BESS configurations, it has been shown that BtM BESS reduces energy curtailments and contributes substantially to resource adequacy as its energy capacity increases. However, the investment feasibility is only ensured if the capacity value of the BtM storage is properly monetized or additional dependability of wind production is claimed on the ground that the inherent intermittency of the wind production is mitigated owing to storage.

Keywords: battery energy storage stations; wind energy; management principle; autonomous power systems; non-interconnected island; renewable penetration; unit commitment; capacity adequacy; economic assessment; mixed integer linear programming



Citation: Dratsas, P.A.; Psarros, G.N.; Papathanassiou, S.A. Feasibility of Behind-the-Meter Battery Storage in Wind Farms Operating on Small Islands. *Batteries* **2022**, *8*, 275.

<https://doi.org/10.3390/batteries8120275>

Academic Editors: Pascal Venet, Karim Zaghib and Seung-Wan Song

Received: 23 September 2022

Accepted: 1 December 2022

Published: 6 December 2022

Publisher's Note: MDPI stays neutral with regard to jurisdictional claims in published maps and institutional affiliations.



Copyright: © 2022 by the authors. Licensee MDPI, Basel, Switzerland. This article is an open access article distributed under the terms and conditions of the Creative Commons Attribution (CC BY) license (<https://creativecommons.org/licenses/by/4.0/>).

1. Introduction

1.1. Motivation

The penetration of intermittent renewable energy sources (RES) in non-interconnected island (NII) power systems is subject to technical and security limitations, hampering their renewable energy hosting capacity ([1]). The main factor that bounds renewable energy absorption levels in NII power systems is its stochastic nature, in conjunction with technical and operational security limitations imposed by the online conventional units [1,2]. Due to these constraints, active power curtailments are imposed on RES stations during the real-time operation of the systems via set-point commands calculated and issued by the NII system operator (NII-SO). The set-point value defines the maximum permissible injection of non-dispatchable RES into the island grid at any given time interval, imposing inevitable curtailments to the RES stations that incorporate set-point receiving functionality. This has a twofold effect on system operation; firstly, an amount of the available RES energy is wasted, and, thus, the power system does not reap the full benefit that RES could potentially provide, while, at the same time, thermal units' share in the generation mixture of NIIs remains significantly high.

Under such circumstances, the deployment of energy storage is a potentially effective means to exploit the otherwise wasted renewable energy and increase the RES hosting capacity of isolated grids, offering a bundle of services to system operation, including frequency regulation [3,4], RES output stability [5,6], active power reserves provision [7], energy arbitrage [8], generation cost reduction [9], etc. However, despite the undoubted benefits of storage on-system operation, the viability of such investments in NIIs is still obscure.

1.2. Literature Review and Research Gap

For NIIs, two basic management designs of energy storage stations (ESS) are met in the relevant literature and real-world applications [10]:

- (a) an ESS coupled with RES within a Hybrid Power Station (HPS) and
- (b) an ESS centrally managed by the NII-SO.

HPSs are aggregate stations, incorporating ESS and intermittent RES units, that operate as a single entity to ensure the dispatchability of the station. HPSs' structure and operating principles are similar to those of Virtual Power Plants (VPPs) ([11,12]), while their application is widely encountered in European islands [13–19]. HPSs qualify as dispatchable renewable plants, as they do not include thermal units, and their operation has been sufficiently analyzed in the literature ([20–28]). HPSs are gradually finding real-world applications [29,30], while the European Commission recently approved a State aid support scheme to promote such investments [31].

On the other hand, under the centrally managed ESS paradigm, storage facilities are installed as discrete entities directly connected to the system, uncorrelated with any specific RES station, and dispatched by the NII-SO in a similar manner to the rest of the generation assets of the system. Centrally managed storage stations receive dispatch orders from the NII-SO for providing energy and reserve products, contributing to system cost minimization and RES maximization objectives and ensuring the fulfillment of security constraints during the generation scheduling processes. The centrally managed storage facilities in island systems have been examined significantly in the relevant literature, with the main focus being on fast-response battery storage [4,7,8,32–34].

Regarding the RES-BtM storage concept, most of the available literature targets applications of large, interconnected power systems rather than islands. This is because the electricity markets of large continental grids are well-established and competitive market procedures, giving opportunities and incentives to market entities, such as RES, to embody storage stations to increase their revenue by actively participating in the provision of multiple products (energy, balancing, etc.). In these cases, the BtM storage is exploited to mitigate the variability of stochastic renewable generation, to reduce penalties from imbalances due to the deviation of day-ahead forecasts and actual wind production [35,36], and to facilitate renewables participation in electricity markets by developing profits maximization strategies [37–41]. Other studies highlight the positive impact of integrating ESS into RES stations on the system's power quality and stability ([42]) by providing out-of-market services such as voltage and frequency regulation, reactive power control, and congestion management [43,44]. Of course, the concept of BtM storage is not unique to RES stations, it being quite common in consumer facilities, with [45–47] or without [48–53] embedded renewable generation. In these use cases, storage aims to minimize the overall electricity cost of the prosumer, applying strategies for the optimal exploitation of available RES energy, demand charge reduction through load curve shaping via peak shaving and load leveling functionalities [46–49,52,53], as well as for the provision of flexibility services to the system and markets [46,48].

On the contrary, the deployment of storage behind the meter of a RES station operating on isolated power systems, being an internal asset of the plant only visible to the station operator for enhancing its performance, has not yet been examined in depth in the relevant literature, as islands are generally missing the business case for such applications.

1.3. Problem Statement, Contributions, and Paper Structure

For NII systems experiencing high-RES saturation conditions, the limitation of renewable production in real-time operation is a means to secure system operation against severe disturbances, leading to inevitable curtailments and the under-exploitation of the available wind or PV regime.

More specifically, in RES-saturated power systems, the NII-SO calculates, per time interval, the RES hosting capacity of the island and effectively distributes it to the renewable plants of the NII via set-point commands, which determine the maximum power output of an individual RES station during the examined time period. Each renewable station receiving a set-point order from the NII-SO is obliged to comply with that order; otherwise, imbalance penalties might occur. The set-point commands are computed and sent by the NII-SO to the RES stations of the island during the real-time operation. If the available generation of the RES plant exceeds the set-point command, a fraction of the station's renewable energy should be spilled. Otherwise, a part of the set-point command will remain unexploited, meaning that the system could potentially absorb increased amounts of RES energy, which are not available at the time examined.

In light of the above, the BtM storage can be used to improve the efficiency of a RES station by better exploiting the wind production exceeding the set-point commands. This can be achieved by charging the BtM storage when RES production exceeds the set-point and discharging it later when the available wind generation cannot fully cover the set-point orders. Apparently, this storage-RES concept does not alter the dispatchability status of the RES unit, which is still perceived as a non-dispatchable asset by the NII-SO, thus significantly differentiating it from the HPS and centrally managed ESS alternatives.

In this context, this paper proposes a holistic approach to approximating the operation of the BtM storage embedded into RES stations in islands, harvesting the system-level benefit that storage could provide, investigating the feasibility of such an investment, and, eventually, determining the optimum sizing of the BtM installation. A wind farm (WF) located in an existing small NII system is used as a study case, whereby the introduction of a Li-ion BESS is contemplated by the WF owner and operator.

Methodologically, the first target of the analysis is to systematically reproduce the set-point commands to be issued to the RES-BtM station. This is achieved by simulating the generation scheduling problem of the island, which is formulated as a mixed integer linear programming (MILP) unit commitment and an economic dispatch (UC-ED) model, to reproduce the set-point orders. Given the set-point orders for every dispatch hour of the year, a "self-dispatch" algorithm is developed to determine the optimum exploitation of the set-points commands by the RES-BESS facility, aiming to minimize curtailments and maximize revenues to the extent possible by the BESS energy and power capacity. Notably, in the simplified electricity market environment of small islands, RES stations are compensated at fixed tariffs, dispensing with complexities related to market participation.

Besides the benefits associated with RES energy exploitation, introducing BtM storage in a stochastic RES station will enhance its contribution to the capacity adequacy of the island power system, which also needs to be quantified and evaluated economically. To this end, a sequential Monte Carlo simulation (SMCS) probabilistic model is developed, incorporating the operation of the BtM storage. The model is used to evaluate the gains in system reliability and the resulting capacity value of storage, using standard metrics such as the loss of load expectation (LOLE) and the expected energy not supplied (EENS). Given the presence of storage behind the meter of the WF, the enhancement of WF's production dependability is also investigated, assuming that storage can potentially enhance the predictability and controllability of the intermittent RES production without, however, altering the non-dispatchable nature of the plant.

Finally, the financial viability of the BtM storage investment is also carried out, considering a multitude of possible revenue streams and aiming at identifying the storage configuration yielding the higher BESS internal rate of return. In the absence of a specific regulatory framework for BtM BESS in NII, the revenue streams of such investment cannot

be well defined on a market-oriented basis. Thus, in this analysis, all the project's quantifiable revenue streams are identified and combined, where suitable, to assess the financial viability of the BtM storage.

The rest of this paper is organized as follows. Section 2 presents the mathematical formulation of the UC-ED model and the self-dispatch algorithm of the WF with BtM storage. In Section 3, the methodology for assessing the contribution of BtM storage to capacity adequacy is developed. The description of the case study follows in Section 4. Section 5 presents the results of the analysis, with the main findings discussed in Section 6. Finally, the main conclusions are summarized in Section 7.

2. Methodology

2.1. UC-ED Mathematical Formulation

A unit commitment and economic dispatch (UC-ED) model is developed to reproduce the management of the NII generation system and to determine the set-point commands issued to the WF. A cost-optimal approach is adopted for the UC-ED model, which is mathematically structured as a MILP problem with hourly time steps and a 24 h look-ahead optimization horizon. The model simulates the generation scheduling process for the NII system and accounts for the techno-economic characteristics of the oil-fired units, the system security criteria by means of active power reserve requirements, as well as the specific restrictions bounding the production of intermittent renewables in real-time, [1].

2.1.1. Objective Function

The objective function to be minimized stands for the total cost of the optimization problem within the examined time horizon and consists of various cost terms (1).

$$\text{obj}^{\text{uc-ed}} = \min \{ C_{\text{var}}^{\text{Thermal}} + C_{\text{su}}^{\text{Thermal}} + C_{\text{sd}}^{\text{Thermal}} + C_{\text{O\&M}}^{\text{Thermal}} + C^{\text{slacks}} \} \quad (1)$$

In more detail, (1) comprises the generation cost of conventional units, which includes their startup cost ($C_{\text{su}}^{\text{Thermal}}$), the shutdown cost ($C_{\text{sd}}^{\text{Thermal}}$), their variable generation cost ($C_{\text{var}}^{\text{Thermal}}$), and their operation and maintenance costs ($C_{\text{O\&M}}^{\text{Thermal}}$). The variable cost is determined from the specific fuel consumption curve and the cost of fuel and CO₂ emission rights, as detailed in [1]. In addition, the objective function includes a cost term assigned to the potential violation of problem constraints (C^{slacks}), realized through slack variables representing the level of deviation from the full satisfaction of a particular constraint of the optimization problem. Such deviations are appropriately penalized to guarantee that constraints are not satisfied only when necessary in order to avoid infeasibilities in the solving process.

2.1.2. Active Power Equilibrium

The energy balance constraint (2) ensures that the total power output of the online thermal ($\sum_u P_{u,t}$) and RES units, wind ($P_{w,t}$), and PV ($P_{pv,t}$) meets the system demand ($P_{L,t}$). In (2), $P_{\text{ens},t}$ represents potential demand curtailments, which might occur during power inadequacy intervals. In (3), the amount of wind production dispatched during a time interval ($P_{w,t}$) is identified, differing from available wind production ($P_{w,t}^a$) by the curtailments imposed ($x_{w,t}$).

$$\sum_u P_{u,t} + P_{w,t} + P_{pv,t} + P_{\text{ens},t} = P_{L,t} \quad (2)$$

$$P_{w,t} + x_{w,t} = P_{w,t}^a \quad (3)$$

2.1.3. Constraints of Thermal Generation Units

The logical commitment status ($st_{u,t}$) of each thermal unit, involving the transitions from the startup ($su_{u,t}$) to shutdown ($sd_{u,t}$) state and vice versa, is imposed by the binary

variables and presented in restrictions (4) and (5). Specifically, (4) excludes the simultaneous startup and shutdown events for a given unit, while (5) defines a startup event as the transition of the commitment status from the offline mode to the operation mode and a shutdown event as the opposite. Constraints (6) and (7) account for the ramp-up (ru_u) and ramp-down (rd_u) rates of thermal units. Constraints (8) and (9) define the envelope within which each unit is allowed to operate when dispatched, considering the maximum ($P_{u,t}^{\max}$) and minimum ($P_{u,t}^{\min}$) power output of each unit.

$$su_{u,t} + sd_{u,t} \leq 1 \quad (4)$$

$$su_{u,t} - sd_{u,t} = st_{u,t} - st_{u,t-1} \quad (5)$$

$$P_{u,t} - P_{u,t-1} \leq ru_u \cdot T^d \cdot st_{u,t} \quad (6)$$

$$P_{u,t-1} - P_{u,t} \leq rd_u \cdot T^d \cdot st_{u,t} + P_{u,t}^{\max} \cdot sd_{u,t} \quad (7)$$

$$P_{u,t} + r_{u,t}^{spin} \leq P_{u,t}^{\max} \cdot st_{u,t} \quad (8)$$

$$P_{u,t} \geq P_{u,t}^{\min} \cdot st_{u,t} \quad (9)$$

2.1.4. Absorption Constraints of Wind Generation

In NII systems, wind production can be subject to real-time limitations, leading to wind curtailments and the under-exploitation of the available regime. These restrictions, also known as set-point orders, are calculated by the NII-SO and distributed to the individual WFs of the island according to the nominal capacity of each. The acceptable wind power injection to the system at any given interval is determined, taking into account the following two limitations.

- The limitation of the minimum load of committed units (10): the available room for the system to accommodate wind power per time interval is restricted by the system demand requirements and the cumulative technical minimum loading of committed units. In other words, wind generation must not force the thermal units to operate below their technical minimum.
- The dynamic limitation (11): wind power injection must not threaten system dynamics and stability. To determine the acceptable quantity of wind power, the empirical coefficient C_D is used, [54,55], while the parameter $l_{w,t}$ stands for the “non-guaranteed” proportion of the available wind production, i.e., the amount of available wind production that may be suddenly lost.

The wind penetration limit eventually applied is the minimum of these two limitations, which is also limited by the total maximum power output of the operating wind capacity, P_W^{tot} (12). In the study case island of this paper, there exists only one WF consisting of a single wind turbine, which receives the entire set-point of the island system (13).

$$P_{W,\max,t}^{\text{ml}} = P_{L,t} - P_{pv,t} - \sum_u (P_u^{\min} \cdot st_{u,t}) \quad (10)$$

$$P_{W,\max,t}^{\text{d}} = \frac{C_D \cdot \sum_u P_u^{\max} \cdot st_{u,t}}{l_{w,t}} \quad (11)$$

$$P_{W,t}^{\text{sp}} = \min \{ P_{W,\max,t}^{\text{ml}}, P_{W,\max,t}^{\text{d}}, P_W^{\text{tot}} \} \quad (12)$$

$$P_{w,t} = \min \{ P_{W,t}^{\text{sp}}, P_{w,t}^{\text{a}} \} \quad (13)$$

2.1.5. Reserve Requirements

Equation (14) determines the spinning reserve requirements of the NII system (rr^{spin}). Constraint (15) ensures that the reserves provided by all thermal units suffice to meet the respective requirements. The $sl_{r,t}$ denotes the slack variable of this constraint. The allocated

active power reserves should suffice to cover any sudden reduction in RES production and load variations within the hour. Parameter $l_{pv,t}$ stands for the “non-guaranteed” proportion of available PV production, while the load variations are taken into account through the empirical coefficient “a”, ranging from 10% to 25% for different NII system sizes.

$$rr^{spin} = l_{w,t} \cdot P_{W,t} + l_{pv,t} \cdot P_{pv,t} + a \cdot (P_{L,t} - P_{pv,t}) \tag{14}$$

$$\sum_u r_{u,t}^{spin} + sl_{r,t} \geq rr^{spin} \tag{15}$$

2.2. Self-Dispatch Algorithm of WF and BtM BESS

The combined operation of the WF and behind-the-meter BESS, illustrated in Figure 1, is governed by a “self-dispatch” algorithm which aims to make best use of the available absorption capability of the island system, i.e., the set-point orders issued to the wind farm, thus maximizing its energy yield. In principle, the BESS will store any WF energy surplus that cannot be directly absorbed by the system for future injection when system conditions permit. Thus, a self-dispatch algorithm can be formulated, whereby BESS is charging when the available wind production exceeds the system set-point order, while it is discharging when the available wind production is lower than the set-point.

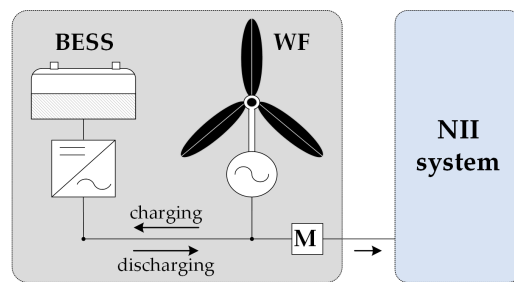


Figure 1. Schematic of WF with embedded BESS.

The self-dispatch algorithm receives, as inputs, the available wind production, the set-point orders on an hourly basis as they are produced by the UC-ED model, and the technical characteristics of the BESS, such as its rated capacity (P_{BESS}^{max}), roundtrip efficiency (η_{BESS}), and state-of-charge (SOC) range limitations (SoC_{min} , SoC_{max}). The algorithm consists of a sequence of logical conditions regarding the relation between the available wind production ($P_{w,t}^a$) and set-point ($P_{W,t}^{SP}$) to determine BESS charging ($P_{ch,t}$) and discharging ($P_{disch,t}$) power. The pseudocode in Table 1 further clarifies the self-dispatch algorithm.

Table 1. Self-dispatch algorithm for the combined operation of WF and BtM BESS.

Self-Dispatch Algorithm	
1:	if ($P_{W,t}^a \leq P_{W,t}^{SP}$) then
2:	$P_{W,t} \leftarrow P_{W,t}^a$
3:	$P_{ch,t} \leftarrow 0$
4:	$P_{disch,t} \leftarrow \min \left\{ P_{BESS}^{max}, (SoC_{t-1} - SoC_{min}) \cdot \sqrt{\eta_{BESS}}, (P_{W,t}^{SP} - P_{W,t}^a) \right\}$
5:	else
6:	$P_{W,t} \leftarrow P_{W,t}^{SP}$
7:	$P_{ch,t} \leftarrow \min \left\{ P_{BESS}^{max}, \frac{SoC_{max} - SoC_{t-1}}{\sqrt{\eta_{BESS}}}, (P_{W,t}^a - P_{W,t}^{SP}) \right\}$
8:	$P_{disch,t} \leftarrow 0$
9:	end
10:	$SoC_t \leftarrow SoC_{t-1} + \sqrt{\eta_{BESS}} \cdot P_{ch,t} - \frac{P_{disch,t}}{\sqrt{\eta_{BESS}}}$

3. Assessment of the Contribution of the BtM BESS to Capacity Adequacy

A Monte Carlo stochastic simulation model, appropriately modified to incorporate the operation of BtM storage, is used to assess the resource adequacy of the NII system. Both the reduction in standard system reliability metrics, LOLE and EENS, due to the introduction of BtM storage, and its capacity value are evaluated to highlight the contribution of BtM storage to adequacy.

3.1. Adequacy Assessment Model

The adequacy assessment model developed in this paper is based on the SMCS technique [56]. Multiple states of the system are sampled by generating random failures of thermal/conventional generation units. A two-state model is developed to reproduce the annual availability realizations of these assets by generating random values of the Time-To-Failure (TTF) and the Time-To-Repair (TTR) variables, following exponential distributions with mean values of $1/\text{MTTF}$ and $1/\text{MTTR}$, respectively, where MTTF represents the mean TTF and MTTR represents the mean TTR. MTTR and MTTF values are used to identify the Forced Outage Rate (FOR) of a generation unit, which in turn expresses the probability of it being out of service. System adequacy is reassessed in every sample s of the SMCS process by measuring the available thermal capacity in hour t ($\text{ATC}_{t,s}$) against the system residual load ($R_{t,s}$) and calculating the reliability metric of LOLE and EENS via (16) and (17), respectively. The $\text{ATC}_{t,s}$ is calculated via (18) for every hour and SMCS sample as the sum of the available capacity of all conventional units; binary parameters $a_{u,t,s}$ stand for the availability of thermal units, determined by the random variables TTF and TTR, and $\text{NGC}_{u,t}$ represents the net generation capacity. The residual load ($R_{t,s}$) is computed by (19) as the load demand ($P_{L,t}$) of the system minus the available PV generation ($P_{pv,t}$) and the output of the combined WF–BESS facility ($P_{t,s}^{\text{WF\&BESS}}$). $P_{pv,t}$ expresses the aggregate power output of the PV stations of the NII system, while $P_{t,s}^{\text{WF\&BESS}}$ represents the power output of the WF that comes from the wind turbine's direct power injection and/or BESS discharging. The calculation of $P_{t,s}^{\text{WF\&BESS}}$ is carried out internally to the SMCS process, taking into account the real-time system capacity needs, and is further described in Section 3.2.

As the number of sample years (N_{MCS}) increases, the EENS converges towards its real value; the SMCS is terminated when the rate of change of EENS between successive steps reaches below 1%.

$$\text{LOLE}_{N_{\text{MCS}}} = \frac{\sum_{s=1}^{N_{\text{MCS}}} \sum_{t=1}^{8760} (R_{t,s} > \text{ATC}_{t,s})}{N_{\text{MCS}}} \quad (16)$$

$$\text{EENS}_{N_{\text{MCS}}} = \frac{\sum_{s=1}^{N_{\text{MCS}}} \sum_{t=1}^{8760} \max(0, R_{t,s} - \text{ATC}_{t,s})}{N_{\text{MCS}}} \quad (17)$$

$$\text{ATC}_{t,s} = \sum_{u \in U} (a_{u,t,s} \cdot \text{NGC}_{u,t}) \quad (18)$$

$$R_{t,s} = P_{L,t} - P_{pv,t} - P_{t,s}^{\text{WF\&BESS}} \quad (19)$$

3.2. Incorporating WF–BESS in the Adequacy Assessment Model

In the context of the adequacy assessment study, the BtM BESS is assumed to operate by pursuing a loss of load minimization objective in order to capture its maximum contribution to system adequacy. Specifically, the BESS absorbs energy whenever there is excess wind production and injects it back into the system when inadequacies appear. This adequacy-oriented storage management, intended to mitigate the loss of load events to the maximum extent, is known as greedy management [57], and it is customary in adequacy assessment studies.

Under this principle, a realistic BESS operation profile is built up according to system capacity needs in real time. The operation of the storage facility is determined within the SMCS process, taking into account the available thermal capacity ($\text{ATC}_{t,s}$), the residual load ($P_{L,t} - P_{pv,t}$) to be served, and the available wind production ($P_{W,t}^a$) while respecting the

BESS technical constraints and the maximum power output of the WF (P_W^{cap}). The algorithm in Table 2 provides the mathematical formulation of the WF and BESS operating algorithm under this concept. Specifically, the following principles apply to the WF–BESS operation in the adequacy assessment methodology:

- If the available thermal capacity ($ATC_{t,s}$) and photovoltaic production ($P_{pv,t}$) suffice to meet the system load ($P_{L,t}$), the available wind production charges BESS to the extent possible (see lines 1–4 in Table 2).
- If the $ATC_{t,s}$ and the $P_{pv,t}$ production do not suffice to satisfy demand, the WF injects power into the system in order to meet the inadequacy (see lines 5–13 in Table 2). In this case, wind power is injected directly from the wind turbine to the grid in order to match the capacity inadequacy if this is possible with respect to the available wind generation ($P_{W,t}^a$) and the WF's cap (P_W^{cap}) (see line 6 in Table 2). If the capacity deficit remains, BESS discharges to contribute to the loss of load mitigation (see lines 7–9 in Table 2). Otherwise, if wind generation exceeds the shortfall, the wind power surplus is used for BESS charging (see lines 10–13 in Table 2).

Table 2. WF–BESS operation algorithm in the framework of adequacy assessment.

WF–BESS Adequacy-Oriented Operation Algorithm	
1:	if ($ATC_{t,s} \geq P_{L,t} - P_{pv,t}$) then
2:	$P_{ch,t,s}^{ad} \leftarrow \min \left\{ P_{BESS}^{max} \cdot a_{t,s}^{BESS}, \frac{(SoC_{max} - SoC_{t-1,s})}{\sqrt{n_{BESS}}}, P_{W,t}^a \right\}$
3:	$P_{disch,t,s}^{ad} \leftarrow 0$
4:	$P_{W,t,s}^{ad} \leftarrow \min \{ P_{W,t}^a - P_{ch,t,s}^{ad}, P_W^{cap} \}$
5:	else
6:	$P_{W,t,s}^{ad} \leftarrow \min \{ P_{W,t}^a, P_W^{cap}, P_{L,t} - P_{pv,t} - ATC_{t,s} \}$
7:	if ($P_{L,t} - P_{pv,t} - ATC_{t,s} > P_{W,t,s}^{ad}$) then
8:	$P_{ch,t,s}^{ad} \leftarrow 0$
9:	$P_{disch,t,s}^{ad} \leftarrow \min \{ P_{BESS}^{max} \cdot a_{t,s}^{BESS}, (SoC_{t-1,s} - SoC_{min}) \cdot \sqrt{n_{BESS}}, P_W^{cap} - P_{W,t,s}^{ad}, P_{L,t} - P_{pv,t} - ATC_{t,s} - P_{W,t,s}^{ad} \}$
10:	else
11:	$P_{ch,t,s}^{ad} \leftarrow \min \left\{ P_{BESS}^{max} \cdot a_{t,s}^{BESS}, \frac{(SoC_{max} - SoC_{t-1,s})}{\sqrt{n_{BESS}}}, P_{W,t}^a - P_{W,t,s}^{ad} \right\}$
12:	$P_{disch,t,s}^{ad} \leftarrow 0$
13:	end
14:	end
15:	$P_{t,s}^{WF\&BESS} \leftarrow P_{W,t,s}^{ad} + P_{disch,t,s}^{ad}$
16:	$SoC_{t,s}^{ad} \leftarrow SoC_{t-1,s}^{ad} + \sqrt{n_{BESS}} \cdot P_{ch,t,s}^{ad} - \frac{P_{disch,t,s}^{ad}}{\sqrt{n_{BESS}}}$

The total output of the combined WF and BESS installation ($P_{t,s}^{WF\&BESS}$) is the sum of wind power injected directly into the grid ($P_{W,t,s}^{ad}$) and BESS discharging power ($P_{disch,t,s}^{ad}$). In addition, the availability of BESS is taken into consideration via the binary variable $a_{t,s}^{BESS}$, which is modeled in a similar manner to the $a_{u,t,s}$ variable. Notably, in the absence of BtM storage, $P_{t,s}^{WF\&BESS}$ equals the available wind production capped by the maximum power output of the WF (P_W^{cap}).

3.3. Capacity Value Estimation of the BtM BESS

The capacity value of BESS is quantified through the equivalent firm capacity (EFC) metric, which denotes the capacity of perfectly reliable generation that would bring about the same adequacy enhancement as the examined BtM BESS configuration.

The EFC metric is computed via an iterative procedure. The base of analysis is the scenario without the BtM BESS, where thermal generation with a zero FOR is gradually added in increments. The process is terminated when the observed EENS becomes equal, as in the scenario with the BtM BESS. EFC is expressed in MW or can be normalized as a

fraction of the BESS rated power capacity. More details on the capacity value calculation method can be found in [34].

4. Study Case

A small NII system with a peak demand of 3.64 MW and a load factor of 33.2% is selected as the study case. The thermal generation comprises eight conventional units of 5.2 MW of total capacity, whose technical characteristics are presented in Table 3. The installed PV capacity is 238 kW, with an annual yield of ~1673 kWh/kW. One WF is in operation on the island, comprising a single 900 kW wind turbine, capped at 665 kW for regulatory purposes. (In small NII systems, the wind hosting capacity is often lower than the size of commercially available wind turbines, leading small wind installations to operate with their output power capped to a level lower than their installed capacity.) The available wind regime at the installation site is sufficient for operation at a capacity factor of 42.8% before cap and curtailments.

Table 3. Main characteristics of the thermal/conventional units of the study case system.

Unit No.	Type	Fuel	P^{\max} [MW]	FOR [%]	MTTR [h]
1–4	ICE ¹	Diesel	1	15%	24
5–8	ICE ¹	Diesel	0.3	20%	24

¹ ICE: Internal Combustion (reciprocating) Engines.

A Li-ion BESS is considered to be installed behind the meter of the WF, with a roundtrip efficiency of 85% and minimum and maximum SoC levels set at 5% and 95%. The FOR of the BtM BESS is assumed at 2%, with an MTTR of 24 h per outage. Several BESS configurations are investigated, including power capacities from 110 to 670 kW and energy capacities ranging from 1 to 6 equivalent hours at rated power.

The optimization UC-ED model is implemented in GAMS [58] using the CPLEX optimizer [59]. The adequacy assessment model is implemented in MATLAB [60] software. A 3.20 GHz Intel Core i7 processor with 16 GB of RAM, running 64 bit Windows, has been used to conduct the simulations.

5. Results and Discussion

5.1. System and WF Operation in the Absence of BtM Storage

The system and the WF operation without BtM storage are presented in Figure 2. In the low-demand and high-wind week, as shown in Figure 2a, curtailments take place during the entire week. The wind power absorption capability of the NII system is low (set-point orders of ~300 kW), while the thermal units operate close to their technical minimum (TM) load to accommodate as much wind production as possible. In the high-demand week of Figure 2b, wind curtailments decrease but still exist, the main reason being the 665 kW constraint imposed on the output power of the 900 kW wind turbine. For low-wind conditions, as shown in Figure 2c,d, curtailments are minimized, and the wind hosting capability of the system remains largely unexploited. Apparently, the exploitation of available wind power strongly depends on the level of load demand.

In the absence of storage, 1442.8 MWh of available wind energy are curtailed annually, corresponding to 42.75% of the available annual wind production. In Table 4, annual curtailments are further analyzed in terms of their origin. The minimum load limitation of committed thermal units and the dynamic limitation are responsible for 95.3% of the curtailed wind energy, while the capacity cap imposed on the WT rarely leads to additional curtailments. The annual time series of curtailments and the unexploited set-point are presented in Figure 3. The lowest curtailments occur in the summer, when demand is high, while the maximum curtailed wind generation is equal to the rated WT power. Wind energy curtailments typically last for many consecutive hours or even days, indicating that very large storage capacities would be required to mitigate them. The unexploited set-point

represents the capability of the system to accommodate wind energy, which is not exploited due to the lack of the coincident availability of wind resources. The annual unexploited set-point is calculated at 716.6 MWh/y.

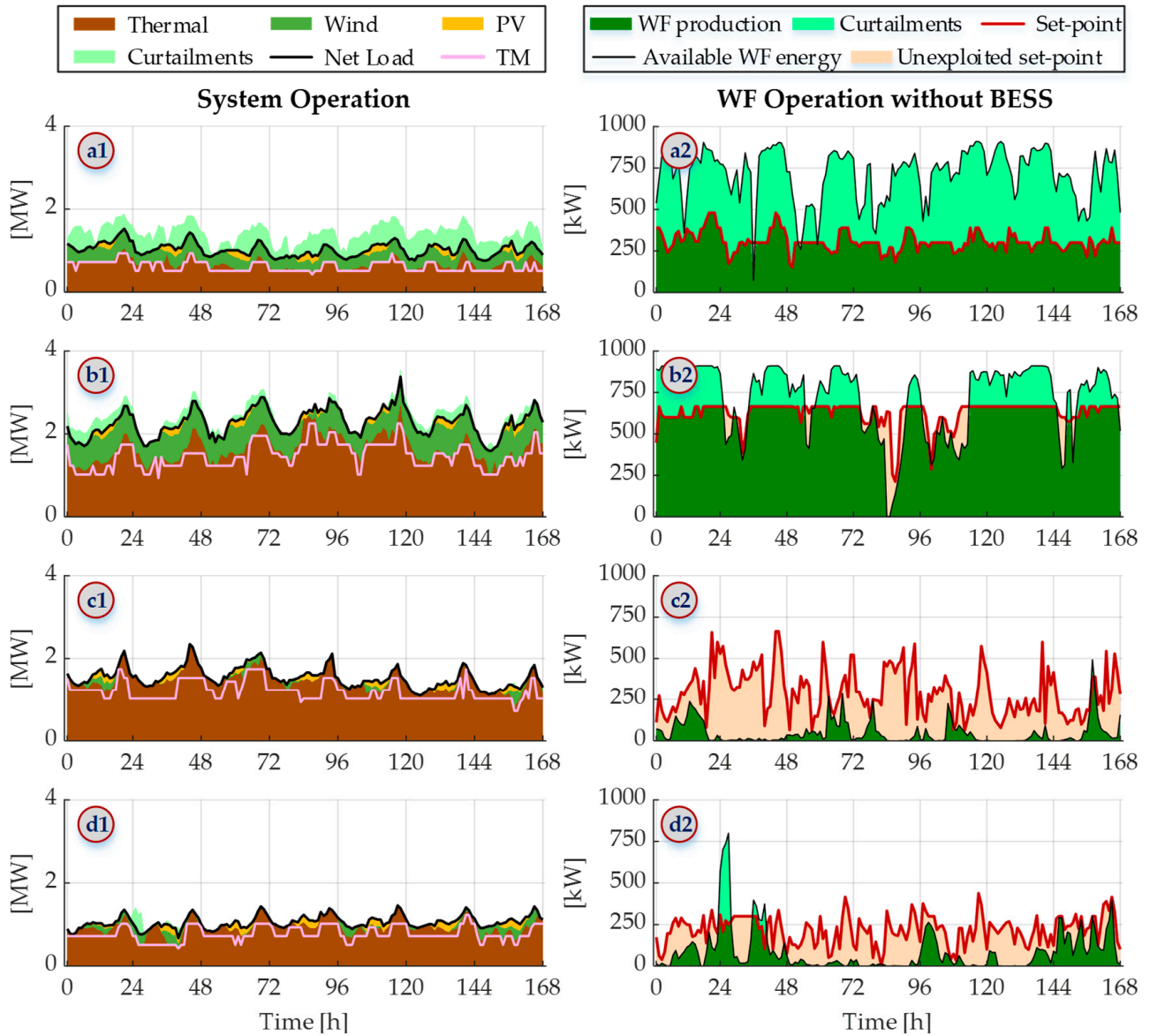


Figure 2. (1) System and (2) WF operation for indicative weeks: (a) low demand and high wind potential, (b) high demand and high wind potential, (c) high demand and low wind potential, (d) low demand and low wind potential.

Table 4. Annual curtailment analysis.

Limitation	Curtailments [MWh]	Duration of Activation		
		[h]	[% of Curtailment Duration]	[% of Year]
Min Load	753.1	2098	48.6%	23.9%
Dynamic	622.3	1851	42.8%	21.1%
WT capacity cap	67.4	372	8.6%	4.2%
Total	1442.8	4321	100.0%	49.3%

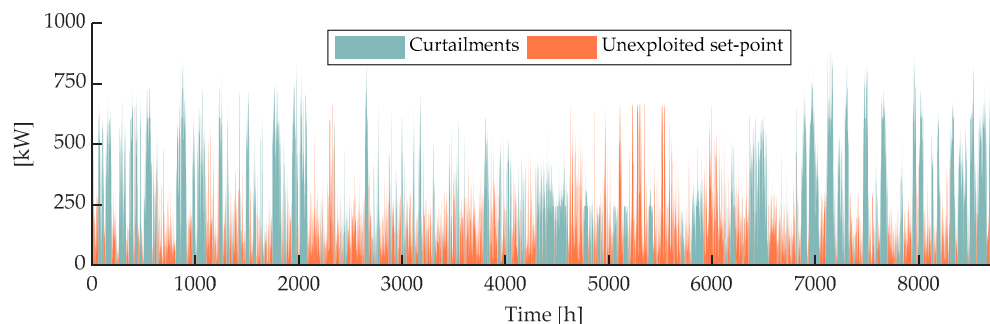


Figure 3. Annual timeseries of curtailments and the unexploited set-point in the no BESS scenario.

The capacity factor of the WF in the no BESS scenario is 24.51%, calculated on the WF’s rated capacity of 900 kW, based on the 1932.4 MWh injected annually to the NII grid. The total RES penetration in the island system is 22.13% of the annual load demand.

Assuming the economic parameters shown in Table 5, the levelized cost of energy (LCOE) of the WF is calculated at EUR 98.77/MWh, which establishes the required Feed-in-Tariff (FiT) for the WF to constitute a viable investment.

Table 5. WF economic parameters.

Investment Cost [EUR/kW]	Tax Rate [%]	O&M Cost [% of CAPEX]	Interest Rate [%]	Depreciation	Evaluation Period [Years]
1400	22.0	3.5	8.0	Linear, 20 years	20

5.2. WF and System Operation following the Introduction of BtM Storage

5.2.1. WF–BESS Operation

The operation of the combined WF–BESS facility is presented in Figures 4 and 5 for indicative weekly intervals and different BESS configurations. In Figure 4, the significance of the energy capacity (duration) of the storage for the effective mitigation of curtailments becomes clear; while the 6 h BESS achieves the improved exploitation of curtailed wind energy compared to the 1 h BESS, it is still evident that an even larger storage capacity would be needed to effectively eliminate rejected wind energy due to the fact that wind curtailments take place over prolonged time intervals, as already noted.

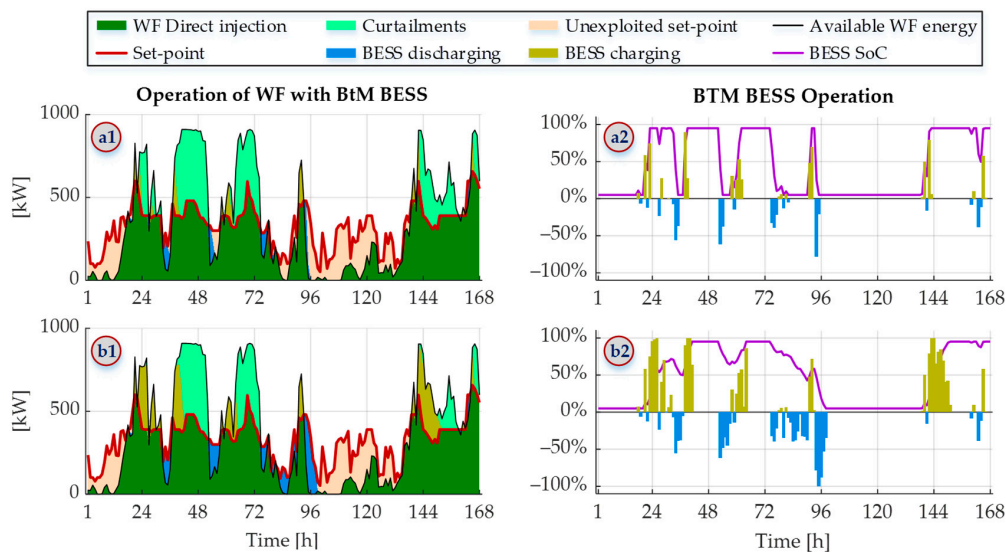


Figure 4. Operation of (1) WF and (2) BtM BESS over an indicative week, assuming (a) 390 kW/1 h (390 kWh) BESS and (b) 390 kW/6 h (2340 kWh) BESS.

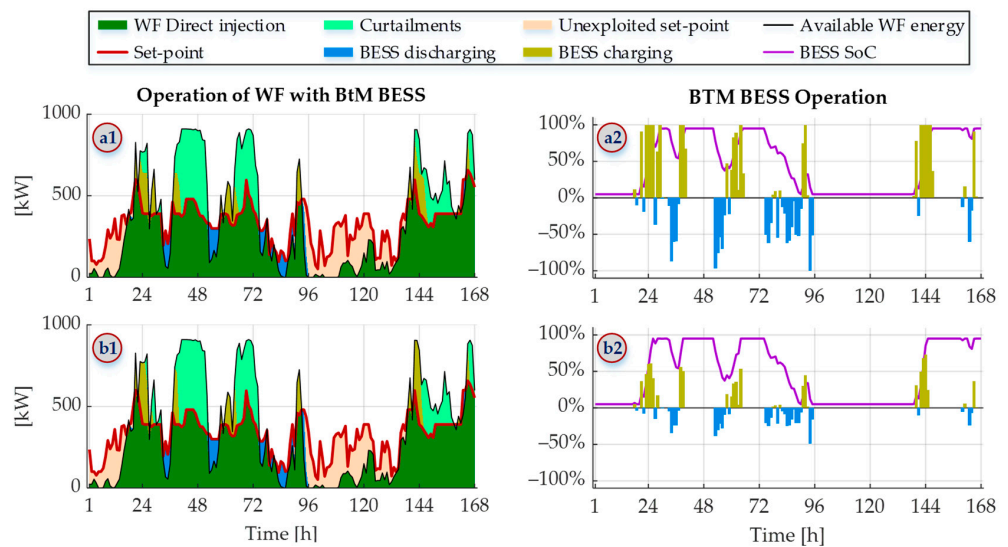


Figure 5. Operation of (1) WF and (2) BtM BESS over an indicative week, assuming (a) 250 kW/5 h (1250 kWh) BESS and (b) 625 kW/2 h (1250 kWh) BESS.

Figure 5 shows that the power rating of the storage does not play a significant role, as, for a given energy capacity (1250 kWh in the diagrams), the gains in wind energy capture are not essential; it is also noted that the installed power capacity of the lower-rated BESS (Figure 5a) is better utilized, while the higher-rated BESS (Figure 5b) operates at fractional capacity levels.

5.2.2. Benefits from the Integration of BtM Storage

Figure 6 shows the reduction in wind power curtailments due to the introduction of storage as a function of BESS rated power (Figure 6a) and energy capacity (Figure 6b). As Figure 6b indicates, the energy capacity of storage is the decisive factor for wind curtailments reduction. A reduction of up to ~22% can be achieved in the level of spilt wind energy, with a corresponding increase in wind energy yield; however, curtailments remain high despite the integration of storage; even for the largest configuration examined (670 kW/6-h), they reach 33.2% (1121 MWh) of the annually available wind energy. The storage capacity needed to fully exploit available wind energy would be unrealistic and infeasible. For instance, to reduce curtailments below 5% of the available wind production, a 670 kW BESS with a duration of approximately 570 h would be required.

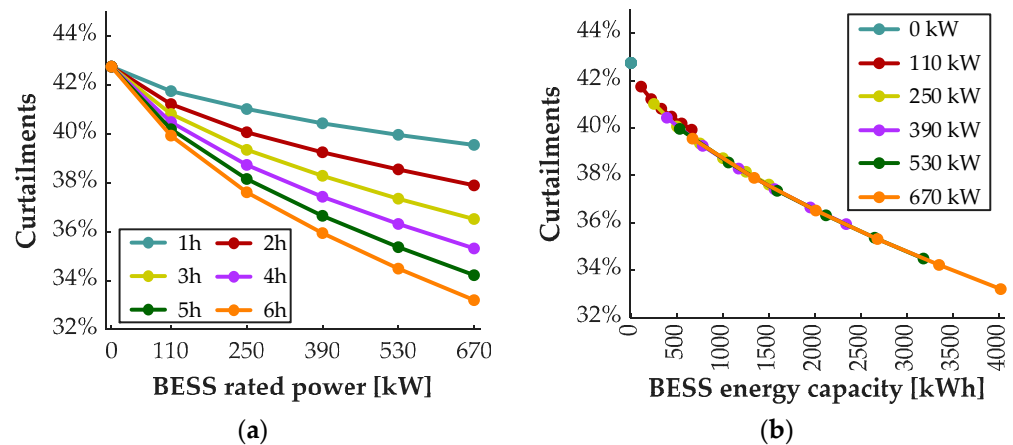


Figure 6. Annual wind energy curtailments as a function of BESS (a) rated power and (b) energy capacity, for different BESS configurations.

The corresponding increase in wind energy output is presented in Figure 7a, while Figure 7b presents the additional revenue of the WF, assuming a FiT of EUR 98.77/MWh, as calculated in Section 5.1. Even for the largest BESS (670 kW/6-h), the economic benefit for the wind producer does not exceed EUR 30 k per annum.

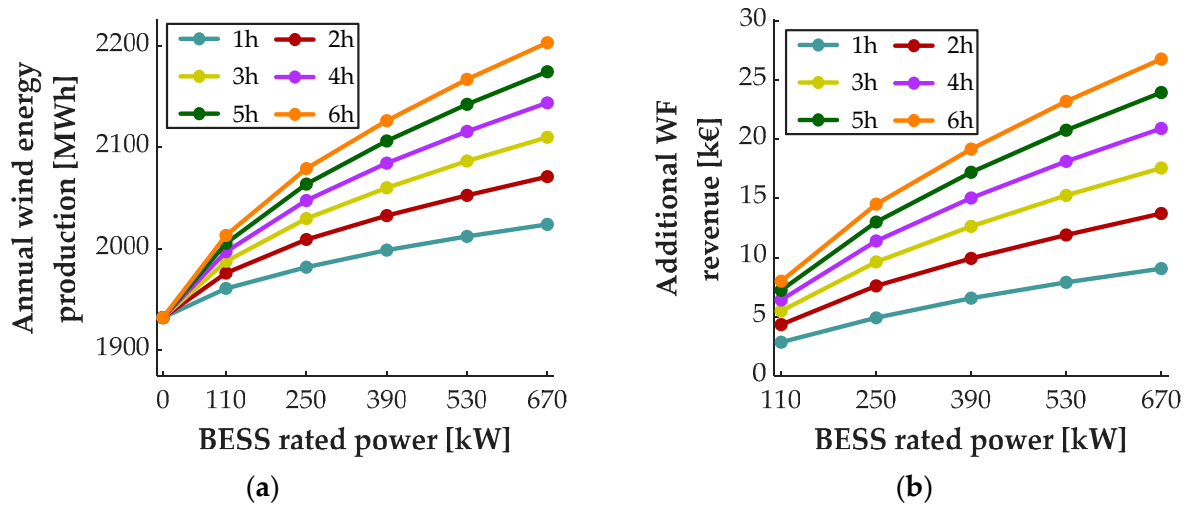


Figure 7. (a) Wind energy injected into the NII system and (b) additional WF revenue due to the introduction of BtM storage for different BESS configurations.

From a system perspective, the resulting annual RES penetration in the island system is presented in Figure 8a, and the impact on annual CO₂ emissions is shown in Figure 8b for all BESS configurations examined. The effect of the storage is positive but far from spectacular, as expected.

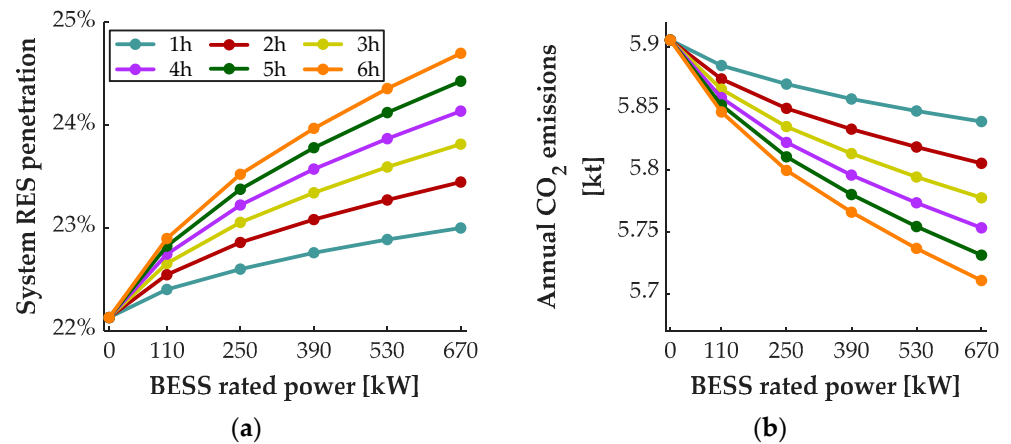


Figure 8. (a) RES penetration, % of annual energy demand of the NII system, and (b) annual CO₂ emissions of conventional units for different BESS configurations.

5.2.3. Contribution of the BtM BESS to Capacity Adequacy

Figure 9 presents the variation in system adequacy, quantified through LOLE and EENS for all storages considered for the WF. In the absence of storage, the LOLE of the NII system reaches 11.17 h, and the EENS is 4.12 MWh (i.e., 0.389% of the annual load demand) per year. The introduction of storage drastically improves system reliability, with EENS and LOLE decreasing by 70% and 75%, respectively, for the largest BESS configuration examined (670 kW/6 h), while smaller storages also achieve a significant reduction in adequacy indices. The energy capacity of the batteries plays an important role in its contribution, as it allows for the improved exploitation of the available power capacity;

however, this positive impact tends to saturate at higher energy capacities. Indicatively, increasing the capacity of a 1 h BESS by an additional 1 h yields a LOLE improvement from 4.1% to 14.7%, depending on the BESS power, while the same increase to a 5 h system will only bring about a LOLE improvement of 1.7% to 3.5%.

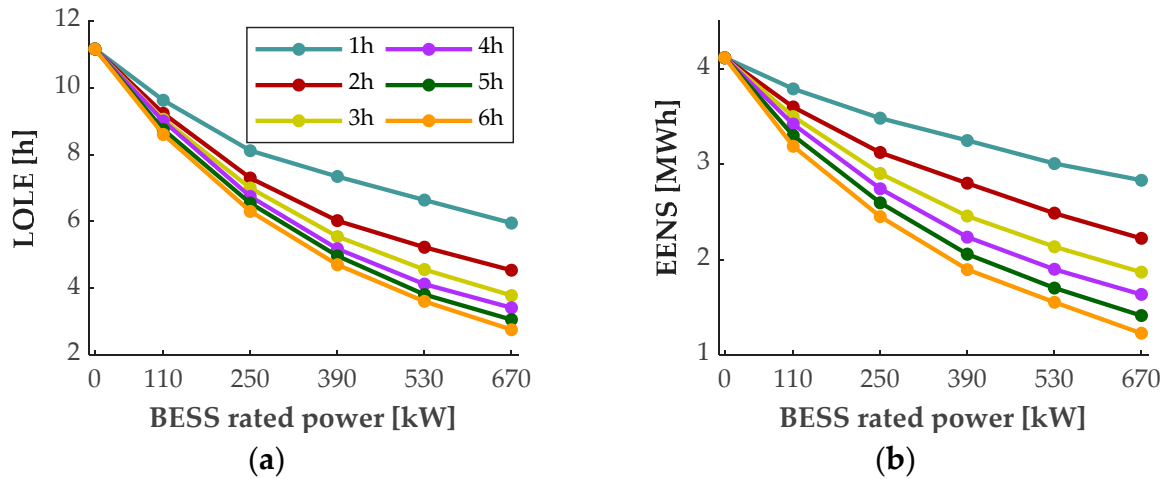


Figure 9. System adequacy results: (a) LOLE; (b) EENS achieved by different BESS configurations.

The capacity value of the examined BtM storage configurations is shown in Figure 10 using the EFC metric, expressed in kW and normalized on the rated power of the batteries. The capacity value of storage corresponds to the improvement in system adequacy due to storage integration compared to the scenario without storage. Apparently, the higher the power and energy capacity of storage, the greater its capacity value, with the energy component having a stronger effect, as demonstrated in Figure 10a. The normalized values, illustrated in Figure 10b, show that the exploitation of BESS power in enhanced adequacy contribution varies significantly for different energy capacities, proving the decisive impact of this characteristic on the contribution of the storage to system reliability [34]. For instance, the EFC of a 250 kW BESS varies between 23.8% and 72.6% with its duration due to the fact that the higher storage energy capacities allow for the more effective exploitation of available BESS power. It is significant to note that the capacity value of a 1 h BESS does not exceed 27.6% at any BESS power level. It is also observed that the normalized capacity value declines at higher BESS powers, reflecting a need for even greater energy capacities at such levels of power.

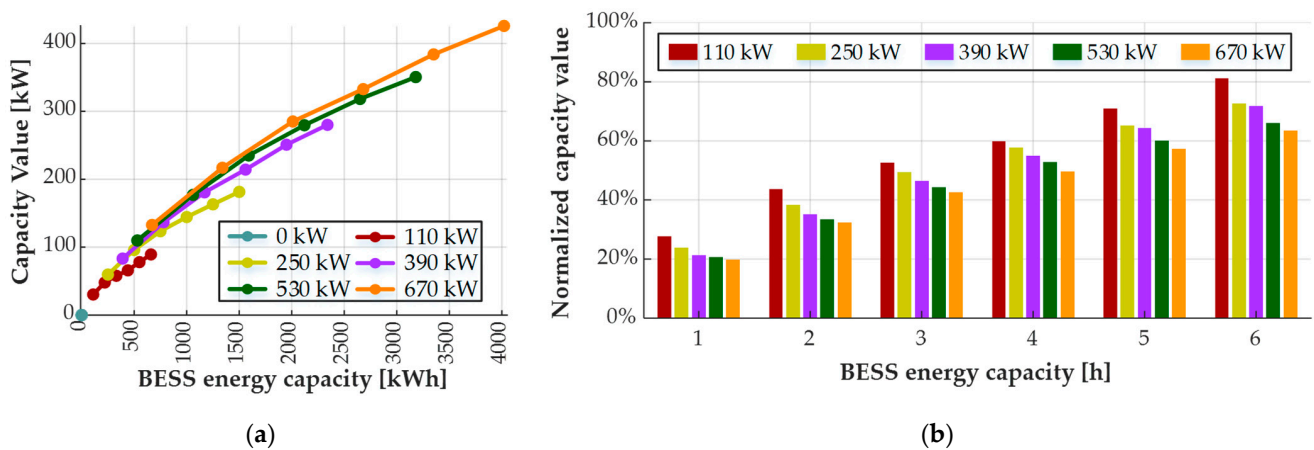


Figure 10. Capacity value of different BESS configurations: (a) in kW and (b) normalized on BESS rated power.

5.2.4. Feasibility Analysis of BESS Investment

In this section, the fundamental question is addressed of whether the integration of BtM storage in the WF makes sense as an investment, based on the additional revenue streams thus created. The feasibility of investment is evaluated on the basis of its project IRR, calculated through (20) [61], where RV represents the annual revenues and I_0^{BESS} represents the initial CAPEX of the batteries. All parameters are provided in Table 6.

$$I_0^{\text{BESS}} + \sum_{t=1}^{20} \frac{(RV_t - OM_t - D_t) \cdot (1 - T) + D_t}{(1 + \text{IRR})^t} = 0 \quad (20)$$

Table 6. BESS economic evaluation parameters.

Investment Cost		Tax Rate (T) [%]	O&M Cost (OM) [% of CAPEX]	Depreciation (D)	Evaluation Period [Years]
BESS Energy [EUR/kWh]	BESS Power [EUR/kW]				
300	120	24.0	3.5	Linear, 20 years	20

The additional revenue due to the integration of storage in the WF, quantified in Section 5.2.2, is not sufficient to ensure the viability of the respective investment, as shown in Figure 11a, leading to negative IRR values. Nevertheless, this additional revenue does reflect the full benefits for the system achieved through the introduction of behind-the-meter storage in the WF. In this vein, the BESS contribution to system adequacy, quantified in Section 5.2.3, corresponds to a substantial avoided cost of investing in equivalent thermal capacity, whose annual fixed cost should, in principle, be credited to the WF incorporating BtM storage. Under this assumption, the IRR of the BESS investment clearly improves, as shown in Figure 11b, where the 110 kW/1 h or 2 h as well as the 250 kW/1 h BESS configurations constitute feasible investments. In this analysis, the annualized equivalent fixed cost of conventional generation is considered at EUR ~177/kW [10].

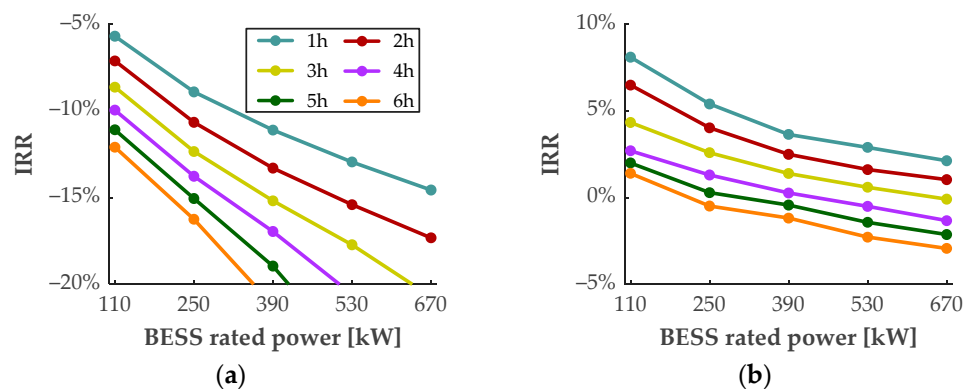


Figure 11. IRR of BESS investment (a) without and (b) with considering additional revenue equal to the value of the BESS contribution to system capacity adequacy, for different BESS configurations.

5.3. Enhancement of System Management

The integration of storage behind the meter of the WF, besides smoothing its variability and allowing for the improved exploitation of set-point orders, may also enhance WF generation dependability, mitigating sudden large reductions in WF output, which can be counteracted by increasing the output power of the battery. Hence, the integration of BtM storage effectively reduces the level of “non-guaranteed” wind generation; this needs to be taken into account by properly modifying the parameter $l_{w,t}$ in (11) and (14), which expresses the non-reliable proportion of available wind power. While, for a single WF without storage, this parameter equals 1, the embedded BESS system will compensate any wind power reduction up to its rated power, allowing for a corresponding reduction in the

value of parameter ($l_{w,t}$). Adopting a reduced value for this parameter will enhance the wind power absorption capability of the system, as the dynamic limitation (11) is relaxed, while the spinning reserve requirements of the system are also reduced in (14). Nevertheless, it should be pointed out that this relaxation may not be possible if the probability of losing all the available wind generation is deemed significant for other reasons besides wind variability, e.g., as a result of external network faults setting out of operation the entire WF, including its BtM BESS. For this reason, the hypothesis of enhanced wind power dependability is addressed as a separate case.

So far, the possibility of BESS enhancing wind production dependability has been disregarded (base scenario). In the following, we take into consideration this possibility, allowing for the relaxation of the dynamic limitation and the reduction in system spinning reserve requirements. As presented in Figure 12, wind energy curtailments are radically reduced when an enhanced WF dependability is adopted.

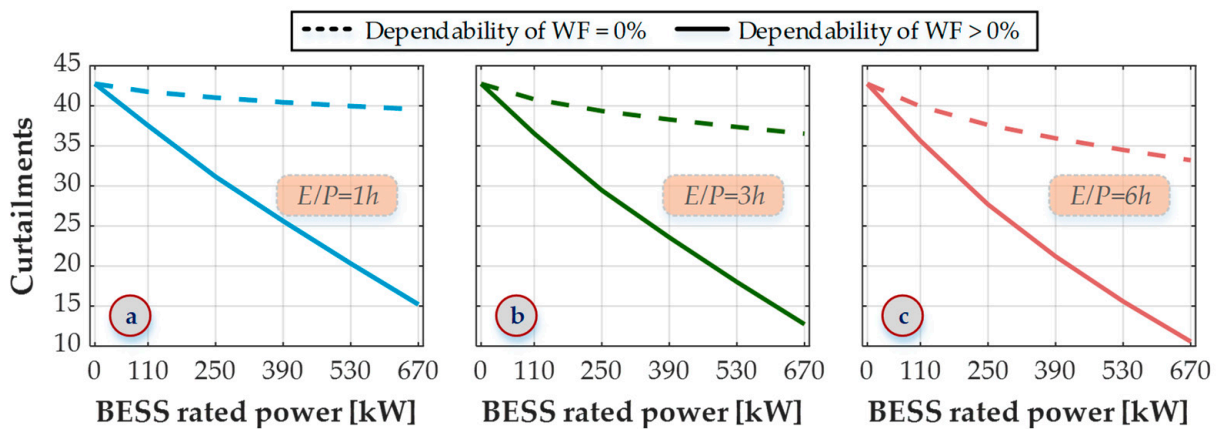


Figure 12. Annual wind energy curtailments, considering or not considering an enhanced WF dependability level, for BESS configurations of (a) 1 h, (b) 3 h, and (c) 6 h durations.

In Figure 13a, the allocation of curtailed wind energy to the applicable system constraints is shown for the BESS of different power capacities. The impact of the dynamic limitation is drastically reduced as more powerful batteries are used, while a marked reduction in the spinning reserve requirements compared to the base scenario is noted in Figure 13b, as the enhanced wind generation dependability, afforded by the introduction of dispatchable storage, poses a need for reduced system reserves (see constraint (14)).

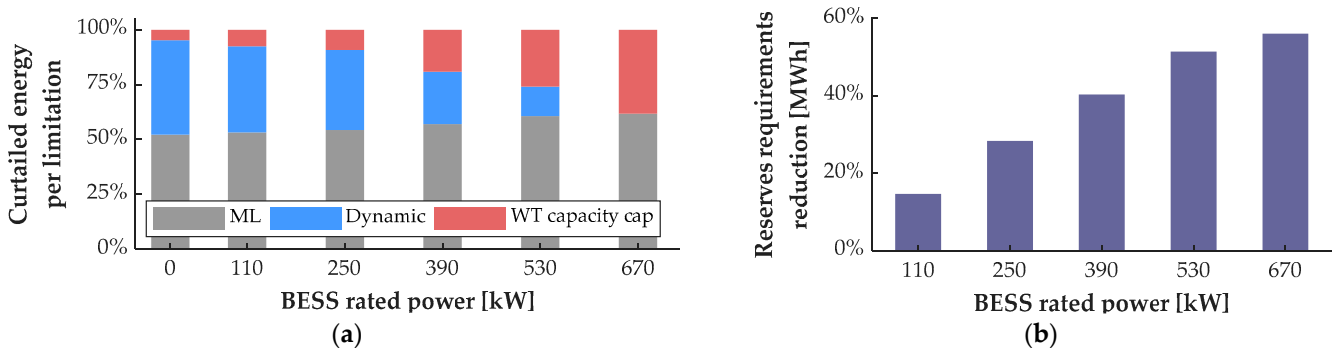


Figure 13. (a) Allocation of curtailments to applicable system constraints and (b) reduction in spinning reserve requirements compared to the base-case scenario for different BESS rated power levels.

As a result of the relaxation of the dynamic limitation, increased set-point values allow greater amounts of wind energy to be injected in the NII system directly, as they are produced by the wind turbine, rather than cycled through its internal storage, as shown in

Figure 14a, where only the BESS rated power matters, rather than its energy capacity. On the other hand, the utilization of the batteries to cycle the excess of wind energy, shown in Figure 14b, presents only marginal differences compared to the base-case scenario due to the fact that the battery capacity barely suffices to manage a minimum level of curtailments that exist regardless of the management policy adopted; only the largest batteries present a noticeable difference, which, again, is not significant. The total wind energy injected into the system on an annual basis for the two management policies and the examined BESS configurations is presented in Figure 15, demonstrating the importance of recognizing the enhancement in wind generation dependability attributed to the introduction of the BtM storage and transposing it into system management.

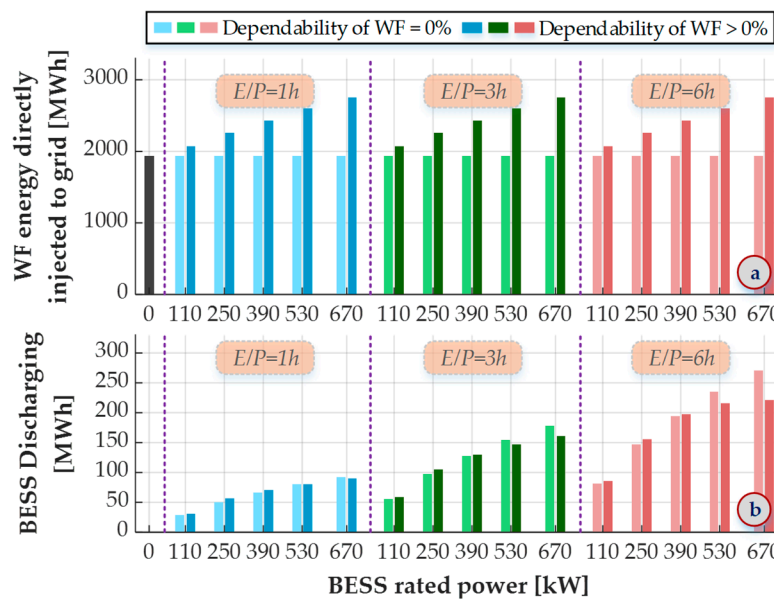


Figure 14. Effect of WF enhanced dependability through the BtM storage. (a) Annual WF energy directly injected to the NII system and (b) annual energy discharge of the BtM BESS, for BESS configurations of 1 h, 3 h, and 6 h durations.

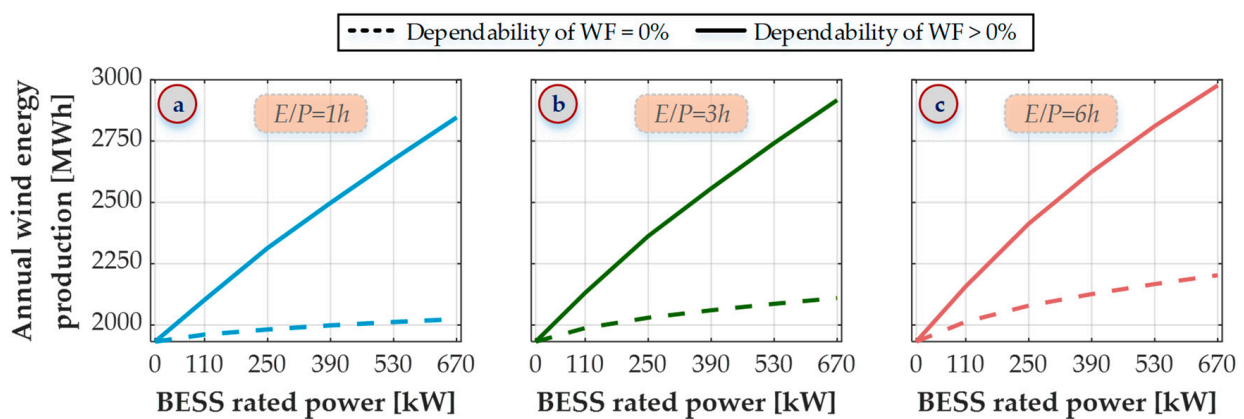


Figure 15. Wind energy injected to the NII system on an annual basis, considering or not considering enhanced WF dependability levels, for BESS configurations of (a) 1 h, (b) 3 h, and (c) 6 h durations.

The investment feasibility analysis is repeated for the amended management policy, and the results are compared in Figure 16 to the base approach. The additional revenue from the increased WF production due to the BESS is now substantial enough to make the investment in BtM storage feasible, even without considering the BESS contribution to adequacy (Figure 16a and even more so if that contribution is accounted for (Figure 16b).

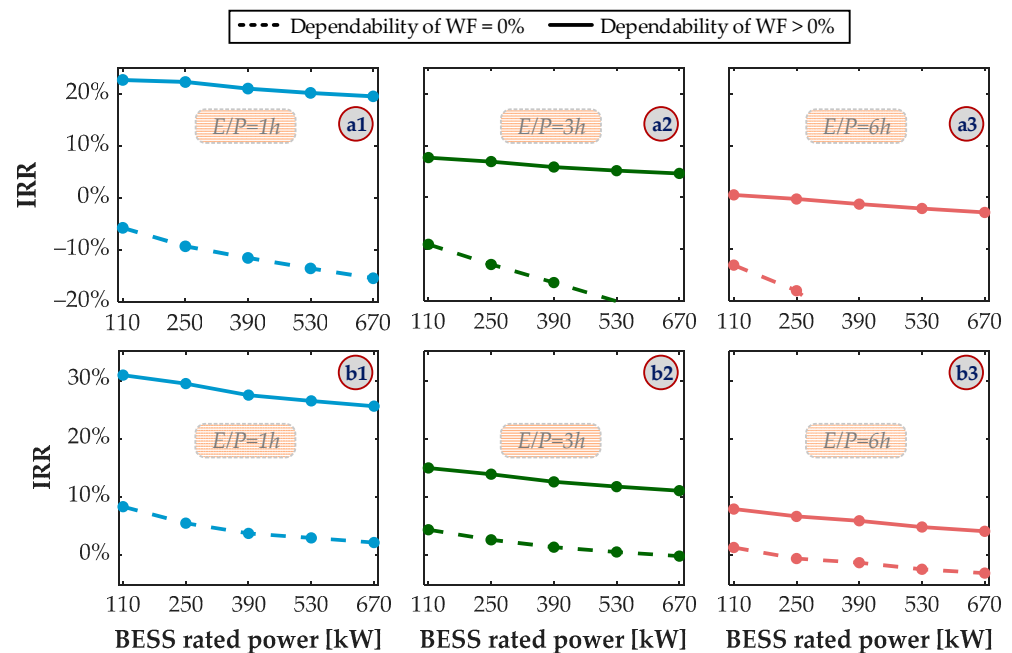


Figure 16. IRR of BESS investment (a) without and (b) with considering the additional revenue reflecting the value of the BESS contribution to capacity adequacy, for (1) 1 h, (2) 3 h, and (3) 6 h BESS configurations.

6. Discussion

The deployment of ESS behind the meter of a RES station constitutes a new concept for storage island applications, which differs significantly from other existing storage paradigms in the literature, i.e., the centrally managed ESS and the HPS. These deployment schemes serve a completely different purpose than the BtM storage, as they primarily aim to increase the RES penetration levels operating as fully dispatchable system assets. At the same time, from a system-level perspective, they might encompass comparative advantages, as, in principle, they provide more services to the grid (energy arbitrage and balancing). However, for the implementation of centrally managed storage and HPS plants in real-world island systems, advanced energy control center infrastructures and complex optimization algorithms are required [7,21], which are not always available in islands, especially to the smaller ones, creating additional obstacles to the fast deployment of such solutions.

On the other hand, the BtM storage concept maintains the non-dispatchable characteristics of the RES station, intending only to enhance the efficiency of the specific RES plant without adopting complex management principles to convert the renewable plant into a dispatchable unit or interacting with the rest of the NII system assets. The BtM storage remains an internal asset of a RES station that facilitates and improves its operation. The investment decision of the BtM storage relies solely on the renewable producer and does not anticipate the development of sophisticated management methodologies or other infrastructure from the side of NII-SO. Additionally, the operating principles of the RES–BtM storage proposed in this paper are based on the exploitation of any set-point commands surplus available for the RES unit, as calculated and issued to the station by the NII-SO, and not the uncontrollable injection of renewable energy into the grid. This framework guarantees that the BtM storage will never threaten the security of the island’s operation, given that the set-point orders are computed by NII-SO responsibility and reflect a feasible RES injection pattern for each renewable station operating on the island.

The analysis results show that the introduction of the BtM storage improves WF operation, reducing wind power curtailments and enhancing the RES penetration of the island system. The energy capacity of BESS seems to be the crucial factor for both cur-

tailment reduction and capacity adequacy enhancement. Despite the reduction in WF curtailments, their elimination was not achievable by the BESS configurations examined in the paper. Notably, to attain the wind curtailment elimination target, it is estimated that energy capacity durations much higher than 6 h are required, which, in turn, indicates the deployment of non-realistic BESS configurations, an assumption entirely out of the context of real-world applications.

Another finding of significant value is that the BtM storage can substantially enhance the contribution of the WF to capacity adequacy, with large duration storages (6 h) claiming capacity values up to 80%. This is quite an important observation, especially when compared to the capacity credit levels attributed to the alternative storage paradigms encountered in islands. For instance, the capacity value of HPS, which by definition incorporates storages of longer durations, lies, at most, in the order of ~90% ([10]), while, for standalone BESS, the respective values of 4 h and 6 h configurations do not exceed 60% and 85% ([34]). These figures show that storage, if suitably utilized to contribute to the resource adequacy of the island, yields a considerable amount of firm capacity, regardless of the station's design it belongs to and the specific management principles it should adhere to.

The feasibility analysis reveals that the BtM BESS is not viable if it solely relies on the additional revenues gained by exploiting the otherwise spilled wind energy. If the storage capacity value were to be remunerated, this situation would change, with BESS systems of 110 kW/1 or 2 h and 250 kW/1 h arising as feasible investments for the specific case study island of this paper. Moreover, if the enhanced dependability of stochastic wind production is taken into consideration in the management of the NII system, the resulting energy benefits are drastically increased, ensuring the economic viability of almost all BESS configurations examined in this study.

7. Conclusions

This paper investigated the benefits anticipated from the integration of battery energy storage behind the meter of a wind farm located in a small NII system, and a feasibility analysis for such an investment was conducted. To this end, the management principles for the operation of the combined WF–BESS facility were proposed, and a self-dispatch algorithm was implemented to best use the WF set-point orders issued by the NII-SO. An analytical UC-ED model dedicated to autonomous island systems was also developed and implemented to reproduce these set-point orders. In addition, the contribution of BtM storage to the capacity adequacy of the system was evaluated using the Monte Carlo technique and by developing an adequacy-oriented strategy for storage operation.

The investigation reveals that the integration of BtM storage in a WF operating on an NII system to better exploit the received set-point orders brings certain operational benefits to both the WF and the entire power system, such as energy curtailments reduction, RES penetration increase, CO₂ emissions reduction, and enhancement of system reliability. Additionally, it was shown that these benefits are amplified if extra dependability is attributed to the wind generation due to the presence of BESS. Finally, the salient conclusion of this investigation is that the enhanced energy revenues of the RES plant due to storage may not suffice to establish investment feasibility, unless the value of capacity firming is monetized in terms of capacity adequacy and/or the enhanced dependability of wind production to reduce operating reserve requirements.

Author Contributions: Conceptualization, P.A.D., G.N.P. and S.A.P.; Data curation, P.A.D., G.N.P. and S.A.P.; Formal analysis, P.A.D.; Funding acquisition, S.A.P.; Investigation, P.A.D. and G.N.P.; Methodology, P.A.D. and G.N.P.; Project administration, S.A.P.; Resources, S.A.P.; Software, P.A.D. and G.N.P.; Supervision, S.A.P.; Visualization, P.A.D.; Writing—original draft, P.A.D.; Writing—review & editing, P.A.D., G.N.P. and S.A.P. All authors have read and agreed to the published version of the manuscript.

Funding: This research was partially funded by the Wind Turbine Repowering in Kythnos (WIRE-K) project supported by the New Energy Solutions Optimized for Islands (NESOI)—European Islands

Facility project. The NESOI project has received funding from the European Union's Horizon 2020 research and innovation program under grant agreement N°864266.

Data Availability Statement: Data sharing is not applicable.

Conflicts of Interest: The authors declare no conflict of interest.

References

1. Psarros, G.N.; Nanou, S.I.; Papaefthymiou, S.V.; Papathanassiou, S.A. Generation Scheduling in Non-Interconnected Islands with High RES Penetration. *Renew. Energy* **2018**, *115*, 338–352. [[CrossRef](#)]
2. Psarros, G.N.; Papathanassiou, S.A. A Unit Commitment Method for Isolated Power Systems Employing Dual Minimum Loading Levels to Enhance Flexibility. *Electr. Power Syst. Res.* **2019**, *177*, 106007. [[CrossRef](#)]
3. Fernández-Guillamón, A.; Sarasúa, J.I.; Chazarra, M.; Viguera-Rodríguez, A.; Fernández-Muñoz, D.; Molina-García, Á. Frequency Control Analysis Based on Unit Commitment Schemes with High Wind Power Integration: A Spanish Isolated Power System Case Study. *Int. J. Electr. Power Energy Syst.* **2020**, *121*, 106044. [[CrossRef](#)]
4. Delille, G.; Francois, B.; Malarange, G. Dynamic Frequency Control Support by Energy Storage to Reduce the Impact of Wind and Solar Generation on Isolated Power System's Inertia. *IEEE Trans. Sustain. Energy* **2012**, *3*, 931–939. [[CrossRef](#)]
5. Sun, C.; Zhang, H. Review of the Development of First-Generation Redox Flow Batteries: Iron-Chromium System. *ChemSusChem* **2022**, *15*, e202101798. [[CrossRef](#)] [[PubMed](#)]
6. Ould Amrouche, S.; Rekioua, D.; Rekioua, T.; Bacha, S. Overview of Energy Storage in Renewable Energy Systems. *Int. J. Hydrogen Energy* **2016**, *41*, 20914–20927. [[CrossRef](#)]
7. Psarros, G.N.; Karamanou, E.G.; Papathanassiou, S.A. Feasibility Analysis of Centralized Storage Facilities in Isolated Grids. *IEEE Trans. Sustain. Energy* **2018**, *9*, 1822–1832. [[CrossRef](#)]
8. Sigrist, L.; Lobato, E.; Rouco, L. Energy Storage Systems Providing Primary Reserve and Peak Shaving in Small Isolated Power Systems: An Economic Assessment. *Int. J. Electr. Power Energy Syst.* **2013**, *53*, 675–683. [[CrossRef](#)]
9. Nikolaidis, P.; Chatzis, S.; Poullikkas, A. Optimal Planning of Electricity Storage to Minimize Operating Reserve Requirements in an Isolated Island Grid. *Energy Syst.* **2020**, *11*, 1157–1174. [[CrossRef](#)]
10. Psarros, G.N.; Dratsas, P.A.; Papathanassiou, S.A. A Comparison between Central- and Self-Dispatch Storage Management Principles in Island Systems. *Appl. Energy* **2021**, *298*, 117181. [[CrossRef](#)]
11. Pudjianto, D.; Ramsay, C.; Strbac, G. Virtual Power Plant and System Integration of Distributed Energy Resources. *IET Renew. Power Gener.* **2007**, *1*, 10–16. [[CrossRef](#)]
12. Mashhour, E.; Moghaddas-Tafreshi, S.M. Bidding Strategy of Virtual Power Plant for Participating in Energy and Spinning Reserve Markets—Part I: Problem Formulation. *IEEE Trans. Power Syst.* **2011**, *26*, 949–956. [[CrossRef](#)]
13. Anagnostopoulos, J.S.; Papantonis, D.E. Simulation and Size Optimization of a Pumped-Storage Power Plant for the Recovery of Wind-Farms Rejected Energy. *Renew. Energy* **2008**, *33*, 1685–1694. [[CrossRef](#)]
14. Caralis, G.; Zervos, A. Analysis of the Combined Use of Wind and Pumped Storage Systems in Autonomous Greek Islands. *IET Renew. Power Gener.* **2007**, *1*, 49–60. [[CrossRef](#)]
15. Caralis, G.; Rados, K.; Zervos, A. On the Market of Wind with Hydro-Pumped Storage Systems in Autonomous Greek Islands. *Renew. Sustain. Energy Rev.* **2010**, *14*, 2221–2226. [[CrossRef](#)]
16. Katsaprakakis, D.A.; Christakis, D.G.; Pavlopoulos, K.; Stamataki, S.; Dimitrelou, I.; Stefanakis, I.; Spanos, P. Introduction of a Wind Powered Pumped Storage System in the Isolated Insular Power System of Karpathos–Kasos. *Appl. Energy* **2012**, *97*, 38–48. [[CrossRef](#)]
17. Katsaprakakis, D. AI Hybrid Power Plants in Non-Interconnected Insular Systems. *Appl. Energy* **2016**, *164*, 268–283. [[CrossRef](#)]
18. Martínez-Lucas, G.; Sarasúa, J.I.; Pérez-Díaz, J.I.; Martínez, S.; Ochoa, D. Analysis of the Implementation of the Primary and/or Inertial Frequency Control in Variable Speed Wind Turbines in an Isolated Power System with High Renewable Penetration. Case Study: El Hierro Power System. *Electronics* **2020**, *9*, 901. [[CrossRef](#)]
19. Fernández-Muñoz, D.; Pérez-Díaz, J.I. Unit Commitment in a Hybrid Diesel/Wind/Pumped-Storage Isolated Power System Considering the Net Demand Intra-Hourly Variability. *IET Renew. Power Gener.* **2021**, *15*, 30–42. [[CrossRef](#)]
20. Kaldellis, J.K.; Kapsali, M.; Kavadias, K.A. Energy Balance Analysis of Wind-Based Pumped Hydro Storage Systems in Remote Island Electrical Networks. *Appl. Energy* **2010**, *87*, 2427–2437. [[CrossRef](#)]
21. Psarros, G.N.; Papathanassiou, S.A. Evaluation of Battery-Renewable Hybrid Stations in Small-Isolated Systems. *IET Renew. Power Gener.* **2020**, *14*, 39–51. [[CrossRef](#)]
22. Fernández-Muñoz, D.; Pérez-Díaz, J.I.; Chazarra, M. A Two-stage Stochastic Optimisation Model for the Water Value Calculation in a Hybrid Diesel/Wind/Pumped-storage Power System. *IET Renew. Power Gener.* **2019**, *13*, 2156–2165. [[CrossRef](#)]
23. Martínez-Lucas, G.; Sarasúa, J.; Sánchez-Fernández, J. Frequency Regulation of a Hybrid Wind–Hydro Power Plant in an Isolated Power System. *Energies* **2018**, *11*, 239. [[CrossRef](#)]
24. Ntomaris, A.V.; Bakirtzis, A.G. Optimal Bidding for Risk-Averse Hybrid Power Station Producers in Insular Power Systems: An MPEC Approach. In Proceedings of the 2017 IEEE PES Innovative Smart Grid Technologies Conference Europe (ISGT-Europe), Turin, Italy, 26–29 September 2017; IEEE: Torino, Italy, 2017; Volume 32, pp. 1–6.

25. Al Alahmadi, A.A.; Belkhier, Y.; Ullah, N.; Abeida, H.; Soliman, M.S.; Khraisat, Y.S.H.; Alharbi, Y.M. Hybrid Wind/PV/Battery Energy Management-Based Intelligent Non-Integer Control for Smart DC-Microgrid of Smart University. *IEEE Access* **2021**, *9*, 98948–98961. [[CrossRef](#)]
26. Sahri, Y.; Belkhier, Y.; Tamalouzt, S.; Ullah, N.; Shaw, R.N.; Chowdhury, M.S.; Techato, K. Energy Management System for Hybrid PV/Wind/Battery/Fuel Cell in Microgrid-Based Hydrogen and Economical Hybrid Battery/Super Capacitor Energy Storage. *Energies* **2021**, *14*, 5722. [[CrossRef](#)]
27. Soliman, M.S.; Belkhier, Y.; Ullah, N.; Achour, A.; Alharbi, Y.M.; Al Alahmadi, A.A.; Abeida, H.; Khraisat, Y.S.H. Supervisory Energy Management of a Hybrid Battery/PV/Tidal/Wind Sources Integrated in DC-Microgrid Energy Storage System. *Energy Rep.* **2021**, *7*, 7728–7740. [[CrossRef](#)]
28. Al Ghaithi, H.M.; Fotis, G.P.; Vita, V. Techno-Economic Assessment of Hybrid Energy Off-Grid System—A Case Study for Masirah Island in Oman. *Int. J. Power Energy Res.* **2017**, *1*, 103–116. [[CrossRef](#)]
29. TILOS Project-Eunice Energy Group. Available online: <http://eunice-group.com/projects/tilos-project/> (accessed on 15 July 2022).
30. Naeras-Ikaria's Hybrid Energy System-PPC Renewables. Available online: <https://ppcr.gr/en/announcements/news/336-naeras-hybrid-energy-system> (accessed on 15 July 2022).
31. European Commission State Aid SA.58482 (2021/N)—Greece Remuneration Scheme of Hybrid Power Stations in NIIs of Greece until 2026, 2021. Available online: https://ec.europa.eu/competition/state_aid/cases1/202220/SA_58482_6071B280-0000-C466-A744-CD54648F7772_42_1.pdf (accessed on 20 September 2022).
32. Thomas, D.; Deblecker, O.; Ioakimidis, C.S. Optimal Design and Techno-Economic Analysis of an Autonomous Small Isolated Microgrid Aiming at High RES Penetration. *Energy* **2016**, *116*, 364–379. [[CrossRef](#)]
33. Vagropoulos, S.I.; Simoglou, C.K.; Bakirtzis, A.G.; Thalassinakis, E.J.; Gigantidou, A. Assessment of the Impact of a Battery Energy Storage System on the Scheduling and Operation of the Insular Power System of Crete. In Proceedings of the 2014 49th International Universities Power Engineering Conference (UPEC), Cluj-Napoca, Romania, 2–5 September 2014. [[CrossRef](#)]
34. Dratsas, P.A.; Psarros, G.N.; Papathanassiou, S.A. Battery Energy Storage Contribution to System Adequacy. *Energies* **2021**, *14*, 5146. [[CrossRef](#)]
35. Castronuovo, E.D.; Usaola, J.; Bessa, R.; Matos, M.; Costa, I.C.; Bremermann, L.; Lugaro, J.; Kariniotakis, G. An Integrated Approach for Optimal Coordination of Wind Power and Hydro Pumping Storage. *Wind Energy* **2014**, *17*, 829–852. [[CrossRef](#)]
36. Tziouvani, L.; Hadjidemetriou, L.; Timotheou, S. Energy Scheduling of Wind-Storage Systems Using Stochastic and Robust Optimization. In Proceedings of the 2022 IEEE Power & Energy Society General Meeting (PESGM), Denver, CO, USA, 17–21 July 2022; Volume 739551, pp. 1–5.
37. Garcia-Gonzalez, J.; de la Muela, R.M.R.; Santos, L.M.; Gonzalez, A.M. Stochastic Joint Optimization of Wind Generation and Pumped-Storage Units in an Electricity Market. *IEEE Trans. Power Syst.* **2008**, *23*, 460–468. [[CrossRef](#)]
38. Yuan, Y.; Li, Q.; Wang, W. Optimal Operation Strategy of Energy Storage Unit in Wind Power Integration Based on Stochastic Programming. *IET Renew. Power Gener.* **2011**, *5*, 194–201. [[CrossRef](#)]
39. Trovato, V.; Kantharaj, B. Energy Storage Behind-the-Meter with Renewable Generators: Techno-Economic Value of Optimal Imbalance Management. *Int. J. Electr. Power Energy Syst.* **2020**, *118*, 105813. [[CrossRef](#)]
40. Ding, H.; Pinson, P.; Hu, Z.; Song, Y. Integrated Bidding and Operating Strategies for Wind-Storage Systems. *IEEE Trans. Sustain. Energy* **2016**, *7*, 163–172. [[CrossRef](#)]
41. Lobato, E.; Sigrist, L.; Ortega, A.; González, A.; Fernández, J.M. Battery Energy Storage Integration in Wind Farms: Economic Viability in the Spanish Market. *Sustain. Energy Grids Netw.* **2022**, *32*, 100854. [[CrossRef](#)]
42. Nieto, A.; Vita, V.; Ekonomou, L.; Mastorakis, N.E. Economic Analysis of Energy Storage System Integration with a Grid Connected Intermittent Power Plant, for Power Quality Purposes. *WSEAS Trans. Power Syst.* **2016**, *11*, 65–71.
43. Nieto, A.; Vita, V.; Maris, T.I. Power Quality Improvement in Power Grids with the Integration of Energy Storage Systems. *Int. J. Eng. Res. Technol.* **2016**, *5*, 438–443.
44. Zafiroopoulos, E.; Christodoulou, C.; Vita, V.; Gonos, I.; Zubieta, E.; Santamaria, G.; Lai, N.B.; Baltas, N.G.; Rodriguez, P. Smart Grid Flexibility Solutions for Transmission Networks with Increased RES Penetration. In Proceedings of the CIGRE Paris Session, Paris, France, 28 August–2 September 2022.
45. Lahnaoui, A.; Stenzel, P.; Linssen, J. Techno-Economic Analysis of Photovoltaic Battery System Configuration and Location. *Appl. Energy* **2018**, *227*, 497–505. [[CrossRef](#)]
46. Mahani, K.; Nazemi, S.D.; Arabzadeh Jamali, M.; Jafari, M.A. Evaluation of the Behind-the-Meter Benefits of Energy Storage Systems with Consideration of Ancillary Market Opportunities. *Electr. J.* **2020**, *33*, 106707. [[CrossRef](#)]
47. Bhattarai, B.P.; Myers, K.S.; Bush, J.W. Reducing Demand Charges and Onsite Generation Variability Using Behind-the-Meter Energy Storage. In Proceedings of the 2016 IEEE Conference on Technologies for Sustainability (SusTech), Phoenix, AZ, USA, 9–11 October 2016; pp. 140–146.
48. Kim, Y.-J.; Del-Rosario-Calaf, G.; Norford, L.K. Analysis and Experimental Implementation of Grid Frequency Regulation Using Behind-the-Meter Batteries Compensating for Fast Load Demand Variations. *IEEE Trans. Power Syst.* **2017**, *32*, 484–498. [[CrossRef](#)]
49. Vejdani, S.; Kline, A.; Totri, M.; Grijalva, S.; Simmons, R. Behind-the-Meter Energy Storage: Economic Assessment and System Impacts in Georgia. In Proceedings of the 2019 North American Power Symposium (NAPS), Wichita, KS, USA, 13–15 October 2019; pp. 1–6.

50. Tsai, C.; Ocampo, E.M.; Beza, T.M.; Kuo, C. Techno-Economic and Sizing Analysis of Battery Energy Storage System for Behind-the-Meter Application. *IEEE Access* **2020**, *8*, 203734–203746. [[CrossRef](#)]
51. Jo, B.-K.; Jung, S.; Jang, G. Feasibility Analysis of Behind-the-Meter Energy Storage System According to Public Policy on an Electricity Charge Discount Program. *Sustainability* **2019**, *11*, 186. [[CrossRef](#)]
52. Wu, D.; Kintner-Meyer, M.; Yang, T.; Balducci, P. Analytical Sizing Methods for Behind-the-Meter Battery Storage. *J. Energy Storage* **2017**, *12*, 297–304. [[CrossRef](#)]
53. Wu, D.; Kintner-Meyer, M.; Yang, T.; Balducci, P. Economic Analysis and Optimal Sizing for Behind-the-Meter Battery Storage. In Proceedings of the 2016 IEEE Power and Energy Society General Meeting (PESGM), Boston, MA, USA, 17–21 July 2016; Volume 2016-Novem. [[CrossRef](#)]
54. Kaldellis, J.K. The Wind Potential Impact on the Maximum Wind Energy Penetration in Autonomous Electrical Grids. *Renew. Energy* **2008**, *33*, 1665–1677. [[CrossRef](#)]
55. Andrianesis, P.; Liberopoulos, G.; Varnavas, C. The Impact of Wind Generation on Isolated Power Systems: The Case of Cyprus. In Proceedings of the 2013 IEEE Grenoble Conference, Grenoble, France, 16–20 June 2013; pp. 1–6.
56. Billinton, R.; Li, W. *Reliability Assessment of Electric Power Systems Using Monte Carlo Methods*; Springer: Boston, MA, USA, 1994; ISBN 978-1-4899-1348-7.
57. Edwards, G.; Sheehy, S.; Dent, C.J.; Troffaes, M.C.M. Assessing the Contribution of Nightly Rechargeable Grid-Scale Storage to Generation Capacity Adequacy. *Sustain. Energy Grids Netw.* **2017**, *12*, 69–81. [[CrossRef](#)]
58. General Algebraic Modeling System (GAMS). Available online: <https://www.gams.com> (accessed on 20 February 2020).
59. IBM CPLEX Optimizer. Available online: <https://www.ibm.com/analytics/cplex-optimizer> (accessed on 20 February 2020).
60. Mathworks-MATLAB and Simulink for Technical Computing. Available online: <https://www.mathworks.com/> (accessed on 20 February 2020).
61. Short, W.; Packey, D.; Holt, T. *A Manual for the Economic Evaluation of Energy Efficiency and Renewable Energy Technologies*; National Renewable Energy Laboratory: Denver, CO, USA, 1995; Volume TP-462-517.